

Revisiting charmonium hybrid spectroscopy

Ri-Qing Qian^{1,2,3,*}, Bing Chen^{4,†} and Xiang Liu^{1,2,5,3,‡}

¹*School of Physical Science and Technology, Lanzhou University, Lanzhou 730000, China*

²*Lanzhou Center for Theoretical Physics, Key Laboratory of Theoretical Physics of Gansu Province,*

Key Laboratory of Quantum Theory and Applications of MoE,

Gansu Provincial Research Center for Basic Disciplines of Quantum Physics, Lanzhou University, Lanzhou 730000, China

³*Research Center for Hadron and CSR Physics, Lanzhou University and Institute of Modern Physics of CAS, Lanzhou 730000, China*

⁴*School of Electrical and Electronic Engineering, Anhui Science and Technology University, Bengbu 233000, China*

⁵*MoE Frontiers Science Center for Rare Isotopes, Lanzhou University, Lanzhou 730000, China*

(Dated: February 17, 2026)

Hadrons with explicit gluonic degrees of freedom, such as charmonium hybrids, are key to understanding nonperturbative behavior of strong interaction, yet they remain experimentally elusive. Within a constituent gluon model treating the hybrid as a $c\bar{c}g$ three-body system with a transverse electric gluon, we predict the masses of the lightest hybrid multiplet ($J^{PC} = 1^{--}, 0^{++}, 1^{+-}, 2^{-+}$) to lie in the range 4.19–4.32 GeV. By analyzing their decay patterns, we provide specific, experimentally testable signatures to guide the search for these exotic states at current and future facilities.

I. INTRODUCTION

Understanding the role of gluonic degrees of freedom in hadron structure is a central challenge in nonperturbative QCD. Hybrid mesons, which contain an explicit gluon excitation in addition to a quark-antiquark pair, offer a unique window into this dynamics, distinct from conventional mesons and baryons.

In the light-flavor sector, the search for hybrids with exotic quantum numbers $J^{PC} = 1^{-+}$ has yielded several candidates, including the $\pi_1(1400/1600)$ [1–12], $\pi_1(2015)$ [13, 14], and the more recent $\eta_1(1855)$ [15, 16]. Lattice QCD and phenomenological models predict masses for light hybrids that are broadly consistent with these observations. However, recent detailed analyses of their decay patterns suggest that the $\pi_1(1600)$ and $\eta_1(1855)$ cannot both be explained as hybrid states [17, 18], challenging a simple interpretation and leaving the identification of light-flavor hybrids as an open question.

Heavy-flavor hybrids, while comparatively less explored [19–25], offer significant theoretical advantages. The large charm quark mass provides a higher energy scale, making perturbative treatments of the gluon more reliable. This facilitates both spectral calculations—where the gluon can be modeled as a constituent particle in a $c\bar{c}g$ system—and decay analyses, where the quark-gluon coupling is more tractable. Furthermore, in addition to the usual selection rules for hybrid decays [26], heavy-quark spin symmetry imposes further constraints on decay patterns. These features make the experimental identification of charmonium hybrids particularly promising.

In this work, we perform a systematic study of charmonium hybrid mesons within a constituent gluon model. The hybrid is treated as a $c\bar{c}g$ three-body system with a transverse electric (TE) mode gluon, from which we calculate the spectrum. We

then evaluate their decay dynamics using the QCD coupling between quarks and gluons, identifying the dominant open-charm channels. Based on these results, we provide specific predictions to guide experimental searches for these elusive states at facilities such as BESIII, Belle II, and the forthcoming Super Tau-Charm Facility.

II. THE CHARMONIUM HYBRID MASS SPECTRUM

A. Gluonic degrees of freedom in hybrids

Unlike conventional mesons, hybrid mesons contain explicit gluonic excitations. Modeling this gluonic degree of freedom is a key theoretical challenge. Several complementary approaches exist, including the flux tube model [19, 27, 28], the QCD string model [29], and the constituent gluon model [30, 31]. In the flux tube picture, the gluonic field in the strong-coupling limit condenses into a collective, string-like configuration between the quarks, approximated by a chain of massive “beads.” The constituent gluon model, by contrast, treats the gluon as a dynamical quasi-particle analogous to a constituent quark.

These pictures are connected in a specific limit. When the flux tube is approximated by a single bead, the hybrid simplifies to a three-body system of quark, antiquark, and bead. This description aligns with both the QCD string model [29] and the constituent gluon model [31]. This single-bead approximation has been shown to accurately reproduce the conventional quarkonium spectrum [19]. Building on this, a three-body hybrid model was recently developed in Ref. [32], where the massive bead is interpreted as a constituent gluon.

Central to this description are the quantum numbers of the gluon. While a free gluon carries $J^{PC} = 1^{--}$, the confined environment alters its effective quantum numbers. The bag model predicts that the lowest gluonic excitation inside a confining cavity is a transverse electric (TE) mode with $J^{PC} = 1^{+-}$ [33]. This is consistent with lattice QCD, which finds that the lightest hybrid multiplet corresponds to a hybrid containing a $j_g = 1$ TE gluon [34, 35]. In this work, we

* qianrq@lzu.edu.cn

† chenbing@ahstu.edu.cn

‡ xiangliu@lzu.edu.cn

TABLE I. The lowest charmonium hybrid multiplet with TE-mode constituent gluon with $j_g = 1$.

J^{PC}	1^{--}	0^{-+}	1^{-+}	2^{-+}
$(l_{c\bar{c}}, S_{c\bar{c}})$	$(0, 0)$	$(0, 1)$	$(0, 1)$	$(0, 1)$

therefore adopt a constituent gluon as a TE mode.

The angular momentum state of such a gluon can be decomposed into transverse and longitudinal components (see Appendix A), with the physical gluon being transverse. Following Ref. [25], the TE and transverse magnetic (TM) gluon states are written compactly as:

$$Y_{j_g, m_g}^{(\xi)}(\theta, \phi) = \sqrt{\frac{2j_g + 1}{4\pi}} D_{m_g, \mu}^{j_g}(\phi, \theta, 0) \chi_{\mu, \lambda}^{(\xi)} \epsilon(\lambda, \hat{n}), \quad (1)$$

where the polarization index $\xi = -1$ denotes a TE gluon and $\xi = +1$ a TM gluon. The coefficients $\chi_{\mu, \lambda}^{(\xi)}$ are given by

$$\chi_{\lambda, \mu}^{(-)} = -\frac{\lambda}{\sqrt{2}} \delta_{\lambda, \mu}, \quad \chi_{\lambda, \mu}^{(+)} = \frac{1}{\sqrt{2}} \delta_{\lambda, \mu}. \quad (2)$$

Using the Wigner rotation property $D_{m_g, \mu}^{j_g}(\phi + \pi, \pi - \theta, 0) = (-1)^{j_g} D_{m_g, -\mu}^{j_g}(\phi, \theta, 0)$, the parity of the TE/TM gluon is

$$P_g = \xi(-1)^{j_g}. \quad (3)$$

When this gluon couples with a quark-antiquark pair to form a hybrid meson, the total parity and charge conjugation are

$$P = \xi(-1)^{j_g + l_{c\bar{c}} + 1}, \quad C = (-1)^{l_{c\bar{c}} + S_{c\bar{c}} + 1}, \quad (4)$$

where $l_{c\bar{c}}$ and $S_{c\bar{c}}$ are the orbital angular momentum and total spin of the $c\bar{c}$ pair, respectively. According to the lattice QCD results [36], the TM gluon may correspond to the higher excited gluon field, such as the Σ_g^{*} and Π_g fields. Therefore, hybrid mesons containing the TM gluon may be difficult to produce in experiments. In this work, we therefore restrict our attention to $c\bar{c}g$ states containing the TE gluon.

B. Mass spectrum

In this work, we consider a TE-mode constituent gluon with $j_g = 1$. For the lowest hybrid multiplet, the $c\bar{c}$ pair is in an $l = 0$ state. As shown in Table I, this yields four states. The 1^{--} state has $c\bar{c}$ spin $S = 1$, while the 0^{-+} , 1^{-+} , and 2^{-+} states also arise from the $S = 1$ configuration¹.

We now calculate the mass spectrum of charmonium hybrids using the constituent gluon model, treating the hybrid as a $c\bar{c}g$ three-body system. The constituent gluon carries quantum numbers $J^{PC} = 1^{+-}$, corresponding to a TE mode with

$j_g = 1$. Following our previous work [32], the non-relativistic Hamiltonian for the system is

$$H = \sum_{i=c, \bar{c}, g} \left(m_i + \frac{p_i^2}{2m_i} \right) + \sum_{i=c, \bar{c}} V_{FT}(r_{ig}) + \sum_{i \neq j} V_{OGE}(r_{ij}) + c_H, \quad (5)$$

where V_{FT} is the confining flux-tube potential between the quark/antiquark and the gluon, and V_{OGE} is the one-gluon exchange potential between the c and \bar{c} . Following the flux tube model [19, 27], the confining potential is linear:

$$V_{FT}(r_{ig}) = -\frac{3}{4} C_{ig} b r_{ig}, \quad (6)$$

with color factor $C_{cg} = C_{\bar{c}g} = -3/2$. The one-gluon exchange potential is

$$V_{OGE}(r_{ij}) = C_{ij} \left(\frac{\alpha_s}{r_{ij}} - \frac{8\pi}{3} \frac{\alpha_s}{m_i m_j} \tilde{\delta}(r_{ij}) \mathbf{s}_i \cdot \mathbf{s}_j \right), \quad (7)$$

where $C_{c\bar{c}} = 1/6$ and $\tilde{\delta}(r) = (\sigma / \sqrt{\pi})^3 e^{-\sigma^2 r^2}$ smears the contact interaction. The spin-dependent part is treated perturbatively.

In Jacobi coordinates, the spin-independent Schrödinger equation becomes

$$\left[\frac{\mathbf{p}_\rho^2}{2m_\rho} + \frac{\mathbf{p}_\lambda^2}{2m_\lambda} + \sum_{i=c, \bar{c}} \left(-\frac{3}{2} \frac{\alpha_s}{r_{ig}} + \frac{9}{8} b r_{ig} \right) + \frac{1}{6} \frac{\alpha_s}{\rho} - c_H \right] \psi_H(\rho, \lambda) = E_H \psi_H(\rho, \lambda), \quad (8)$$

where ρ is the relative coordinate between c and \bar{c} , λ is the coordinate between the gluon and the $c\bar{c}$ center of mass, and the reduced masses are $m_\rho = m_c/2$ and $m_\lambda = 2m_c m_g / (2m_c + m_g)$.

The wave function $\psi_H \equiv \psi_{n_\lambda, l_\rho, m_\rho}^{l_\lambda, m_\lambda}(\rho, \lambda)$ is an eigenstate of orbital angular momenta l_ρ and l_λ . To preserve the constituent gluon's 1^{+-} assignment, we restrict to the ground state in the λ -mode ($l_\lambda = 0$) and solve variationally using a simple harmonic oscillator trial wave function:

$$\psi_{0,0}^{00,00}(\rho, \lambda) = \frac{\beta_\rho^{3/2}}{\pi^{3/4}} e^{-\frac{\beta_\rho^2 \rho^2}{2}} \frac{\beta_\lambda^{3/2}}{\pi^{3/4}} e^{-\frac{\beta_\lambda^2 \lambda^2}{2}}. \quad (9)$$

The spin-dependent potentials yield mass shifts for the four $l = 0$ states:

$$\Delta m_{1^{--}} = \frac{3}{4} \zeta, \quad \Delta m_{0^{-+}} = -2\epsilon - \frac{1}{4} \zeta, \quad (10)$$

$$\Delta m_{1^{-+}} = -\epsilon - \frac{\zeta}{4}, \quad \Delta m_{2^{-+}} = \epsilon - \frac{\zeta}{4}, \quad (11)$$

where

$$\epsilon = \langle \psi_H | \frac{4\alpha_s}{\sqrt{\pi}} \frac{\sigma^3}{m_c m_g} e^{-\sigma^2 r_i^2} | \psi_H \rangle, \quad (12)$$

$$\zeta = \langle \psi_H | \frac{4\alpha_s}{9\sqrt{\pi}} \frac{\sigma^3}{m_c^2} e^{-\sigma^2 \rho^2} | \psi_H \rangle. \quad (13)$$

The mass splitting between the 1^{--} and the 0^{-+} , 1^{-+} , 2^{-+} states arises from $c\bar{c}$ spin-dependent interactions, while the splittings among the 0^{-+} , 1^{-+} , and 2^{-+} states originate from spin-dependent quark-gluon interactions.

¹ The 1^{-+} state carries exotic quantum numbers not accessible to conventional $c\bar{c}$ mesons, providing a clear experimental signature.

TABLE II. Parameters used in the spectrum calculation

m_c	m_g	α_s	b	c_H	σ
1.52 GeV	1.05 GeV	0.28	0.132 GeV^2	0.58 GeV	1.30 GeV

Using the variational wave function, these matrix elements evaluate to

$$\epsilon = \frac{4\alpha_s}{\sqrt{\pi}} \frac{\sigma^3}{m_c m_g} \frac{8\beta_\lambda^3 \beta_\rho^3}{(4\sigma^2 \beta_\rho^2 + 4\beta_\lambda^2 \beta_\rho^2 + \beta_\lambda^2 \sigma^2)^{3/2}}, \quad (14)$$

$$\zeta = \frac{4\alpha_s}{9\sqrt{\pi}} \frac{\sigma^3}{m_c^2} \frac{\beta_\rho^3}{(\beta_\rho^2 + \sigma^2)^{3/2}}. \quad (15)$$

The parameters used in the calculation are listed in Table II. They are standard values in the literature for heavy quark systems, chosen to reproduce the known charmonium spectrum [19]. The resulting masses for the lowest hybrid multiplet are

$$\begin{aligned} m_{0^{++}} &= 4.189 \text{ GeV}, & m_{1^{+-}} &= 4.231 \text{ GeV}, \\ m_{1^{--}} &= 4.276 \text{ GeV}, & m_{2^{+-}} &= 4.316 \text{ GeV}. \end{aligned}$$

The spectrum is shown in Fig. 1 alongside relevant open-charmed meson-pair thresholds.

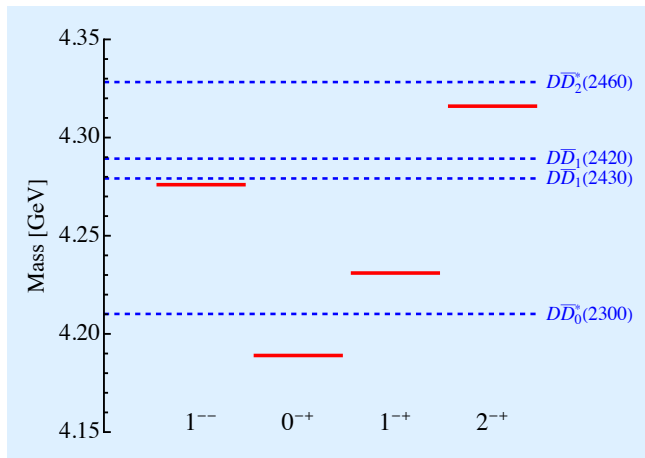


FIG. 1. The lowest $c\bar{c}g$ hybrid multiplet spectrum and charmed meson pair mass thresholds.

III. OPEN CHARM DECAY OF CHARMONIUM HYBRID

A. Decay mechanism

The decay of hybrid mesons is governed by the QCD coupling between quarks and gluons. To leading order in perturbation theory, the interaction Hamiltonian in the interaction picture is

$$H_I = g \int d^4 x \bar{\psi}(x) \gamma^\mu \frac{\lambda_a}{2} \psi(x) A_\mu^a(x), \quad (16)$$

where g is the strong coupling constant, λ_a are the Gell-Mann matrices, and ψ and A_μ^a represent the quark and gluon fields, respectively.

Expanding the field operators in terms of creation and annihilation operators yields the non-relativistic reduction

$$\begin{aligned} H_I &= g \sum_{s,s'} \int \frac{d^3 p \, d^3 p' \, d^3 k}{\sqrt{2\omega_k} (2\pi)^{9/2}} (2\pi)^4 \delta^{(4)}(p + p' - k) \\ &\quad \times \frac{1}{\sqrt{2E_p} \sqrt{2E_{p'}}} \bar{u}_p^s \gamma_\mu \frac{\lambda^a}{2} v_{p'}^{s'} b_{p,s}^\dagger d_{p',s'}^\dagger a_{k,a,\lambda} \epsilon^\mu(\lambda, \mathbf{k}), \end{aligned} \quad (17)$$

where the single-particle states are normalized as $\langle \mathbf{p}, s | \mathbf{p}', s' \rangle = \delta^{(3)}(\mathbf{p} - \mathbf{p}') \delta_{ss'}$. In the non-relativistic limit, the Dirac spinor matrix element simplifies to

$$\frac{1}{\sqrt{2E_p} \sqrt{2E_{p'}}} \bar{u}_p^s \gamma_\mu v_{p'}^{s'} \epsilon^\mu(\lambda, \mathbf{k}) \approx -\chi_s^\dagger \sigma \tilde{\chi}_{s'} \cdot \boldsymbol{\epsilon}(\lambda, \mathbf{k}), \quad (18)$$

where χ_s is the quark Pauli spinor and $\tilde{\chi}_{s'} = -i\sigma_2 \chi_{s'}^*$ represents the antiquark spinor.

A hybrid meson state with definite angular momentum is constructed by coupling the gluon angular wave function from Eq. (1) with the quark-antiquark spatial and spin wave functions. In second-quantized form,

$$\begin{aligned} &|JM[LS]j_g\xi\rangle \\ &= \frac{1}{2} T_{ij}^A \int d^3 p_1 d^3 p_2 d^3 p_g \delta^{(3)}(\mathbf{p}_1 + \mathbf{p}_2 + \mathbf{p}_g) \Psi_{j_g,lm_l}(\mathbf{q}, k) \\ &\quad \times \sqrt{\frac{2j_g + 1}{4\pi}} D_{m_g, \mu}^{j_g*}(\hat{\mathbf{k}}) \chi_{\mu, \lambda}^{(\xi)}(\frac{1}{2}m, \frac{1}{2}\bar{m}|S M_S) \\ &\quad \times \langle lm_l, j_g m_g | LM_L \rangle \langle S M_S, LM_L | JM \rangle \\ &\quad \times b_{p_1, i, m}^\dagger d_{p_2, j, \bar{m}}^\dagger a_{p_g, A, \lambda}^\dagger |0\rangle, \end{aligned} \quad (19)$$

where $\frac{1}{2} T_{ij}^A$ is the color wave function. The normalization condition $\langle JM[LS]j_g\xi | JM[LS]j_g\xi \rangle = \delta^{(3)}(0)$ requires

$$\int d^3 q \, dk \, k^2 |\Psi_{j_g,lm_l}(\mathbf{q}, k)|^2 = 1. \quad (20)$$

Conventional meson states with total momentum \mathbf{P} are similarly constructed:

$$\begin{aligned} &|\mathbf{P}, J_B M_{J_B}\rangle \\ &= \frac{1}{\sqrt{3}} \int d^3 p_1 d^3 p_2 \delta^{(3)}(\mathbf{p}_1 + \mathbf{p}_2 - \mathbf{P}) \phi_{L_B, M_{L_B}}(\mathbf{p}) \\ &\quad \times \langle \frac{1}{2}m, \frac{1}{2}m' | S_B M_{S_B} \rangle \\ &\quad \times \langle S_B M_{S_B}; L_B M_{L_B} | J_B M_{J_B} \rangle b_{p_1, i, m}^\dagger d_{p_2, i, m'}^\dagger |0\rangle, \end{aligned} \quad (21)$$

with the spatial wave function normalized as $\int d^3 p |\phi(\mathbf{p})|^2 = 1$.

The matrix element for the decay $H \rightarrow B + C$ is defined by

$$\langle B(\mathbf{P}) C(-\mathbf{P}) | H_I | H \rangle = (2\pi) \delta^{(4)}(P_H - P_B - P_C) \mathcal{M}^{M_J, M_{J_B}, M_{J_C}}(\mathbf{P}), \quad (22)$$

where the reduced amplitude takes the form

$$\begin{aligned}
\mathcal{M}^{MM_{J_B}M_{J_C}}(\mathbf{P}) &= -\frac{2}{3} \frac{g}{(2\pi)^{3/2}} \int d^3k d^3q \Psi_{j_g,lm_l}(\mathbf{q}, k) \sqrt{\frac{2j_g+1}{4\pi}} D_{m_g,\mu}^{j_g*}(\hat{\mathbf{k}}) \chi_{\mu,\lambda}^{(\xi)} \\
&\times \langle \frac{1}{2}m; \frac{1}{2}\bar{m} | S M_S \rangle \langle lm_l; j_g m_g | LM_L \rangle \langle S M_S; LM_L | JM \rangle \\
&\times \frac{1}{\sqrt{2\omega_k}} \chi_s^\dagger \sigma \tilde{\chi}_{s'} \cdot \epsilon(\lambda, \mathbf{k}) \\
&\times \phi_{L_B M_{L_B}}^* \left(\mathbf{q} - \frac{\mathbf{k}}{2} - \frac{m_c}{m_q + m_c} \mathbf{P} \right) \langle \frac{1}{2}m; \frac{1}{2}s' | S_B M_{S_B} \rangle \\
&\times \langle S_B M_{S_B}; L_B M_{L_B} | J_B M_{J_B} \rangle \\
&\times \phi_{L_C M_{L_C}}^* \left(\mathbf{q} + \frac{\mathbf{k}}{2} - \frac{m_c}{m_q + m_c} \mathbf{P} \right) \langle \frac{1}{2}s; \frac{1}{2}\bar{m} | S_C M_{S_C} \rangle \\
&\times \langle S_C M_{S_C}; L_C M_{L_C} | J_C M_{J_C} \rangle. \tag{23}
\end{aligned}$$

The prefactor $2/3$ arises from the color wave function overlap, and $g/(2\pi)^{3/2}$ follows from our normalization conventions (see Appendix B).

The spin matrix element can be expressed in terms of a Wigner D -function (see Appendix C):

$$\chi_s^\dagger \sigma \tilde{\chi}_{s'} \cdot \epsilon(\lambda, \mathbf{k}) = -\sqrt{2}^{|s+s'|} D_{s+s',\lambda}^1(\hat{\mathbf{k}}). \tag{24}$$

For a $j_g = 1$ TE gluon ($\xi = -1$), combining this with the gluon angular wave function yields

$$\begin{aligned}
&\sqrt{\frac{2j_g+1}{4\pi}} D_{m_g,\mu}^{j_g*}(\hat{\mathbf{k}}) \chi_{\mu,\lambda}^{(\xi)} \chi_s^\dagger \sigma \tilde{\chi}_{s'} \cdot \epsilon(\lambda, \mathbf{k}) \\
&= -\sqrt{2}^{|s+s'|} (-1)^{s+s'} \langle 1m_g; 1 - (s+s') | 1m_{l_g} \rangle Y_{1,m_{l_g}}(\hat{\mathbf{k}}), \tag{25}
\end{aligned}$$

where $Y_{1,m_{l_g}}(\hat{\mathbf{k}})$ represents the angular distribution of the constituent gluon.

The integral over the direction $\hat{\mathbf{k}}$ in Eq. (23) involves the factor $\phi_B^*(\mathbf{k}, \mathbf{P}) \phi_C^*(\mathbf{k}, \mathbf{P}) Y_{1,m_{l_g}}(\hat{\mathbf{k}})$. If the two final-state mesons B and C have identical spatial wave functions, the product $\phi_B^* \phi_C^*$ is even under $\mathbf{k} \rightarrow -\mathbf{k}$, while $Y_{1,m_{l_g}}(\hat{\mathbf{k}})$ is odd. The angular integral therefore vanishes. This leads to a key selection rule: a $j_g = 1$ TE hybrid cannot decay into two mesons with identical spatial wave functions [25]. This selection rule, also found in other hybrid decay analyses [26], has important phenomenological consequences for charmonium hybrid decays.

To compare with experimental observables, we project the decay amplitude onto partial waves using the Jacob-Wick formula. Choosing the final-state momentum along the z -axis, the partial wave amplitude is

$$\begin{aligned}
\mathcal{M}^{S_{BC}L_{BC}}(P) &= \frac{\sqrt{4\pi(2L_{BC}+1)}}{2J+1} \sum_{M_{J_B}, M_{J_C}} \langle L_{BC}0; S_{BC}M | JM \rangle \\
&\times \langle J_B M_{J_B}; J_C M_{J_C} | S_{BC}M \rangle \mathcal{M}^{MM_{J_B}M_{J_C}}(P_z), \tag{26}
\end{aligned}$$

where S_{BC} and L_{BC} are the total spin and orbital angular momentum of the two-meson system. The corresponding partial width is

$$\Gamma^{S_{BC}L_{BC}}(H \rightarrow BC) = 2\pi \frac{E_B E_C}{M_H} P |\mathcal{M}^{S_{BC}L_{BC}}|^2, \tag{27}$$

with $P = |\mathbf{P}|$ the magnitude of the final-state momentum in the rest frame of the hybrid. The total width is obtained by summing over all allowed partial waves and decay channels (see Appendix D).

B. Numerical results

The selection rule derived in the previous subsection has profound implications for the decay patterns of charmonium hybrids with a $j_g = 1$ TE gluon. As established, decays to two mesons with identical spatial wave functions are forbidden. Consequently, the $D\bar{D}$ and $D^*\bar{D}^*$ channels are strictly prohibited. Furthermore, since the D and D^* mesons are both S -wave $c\bar{q}$ states with very similar spatial wave functions, the decay to $D\bar{D}^*$ is strongly suppressed, though not absolutely forbidden. Therefore, the dominant decay modes for these hybrids, when kinematically allowed, are expected to be into an S -wave plus a P -wave meson pair (e.g., $D\bar{D}_0^*$, $D\bar{D}_1$, $D\bar{D}_2^*$). If the hybrid mass lies below all $S + P$ thresholds, the state should be narrow.

For the numerical calculation of decay widths, we require explicit forms for the hybrid and meson wave functions. The hybrid spatial wave function for the lowest multiplet is of the form:

$$\psi_{0,0}^{0,0;1m_{l_g}}(\mathbf{p}_\rho, \mathbf{p}_\lambda) = \frac{\sqrt{8/3}}{\pi^{3/4} \beta_\rho^{2/3} \pi^{1/4} \beta_\lambda^{5/2}} p_\lambda Y_{1,m_{l_g}}(\hat{\mathbf{p}}_\lambda) e^{-p_\rho^2/2\beta_\rho^2 - p_\lambda^2/2\beta_\lambda^2},$$

where β_ρ and β_λ are the oscillator parameters obtained from the spectrum calculation.

The conventional meson wave functions are approximated by simple harmonic oscillator (SHO) wave functions:

$$R_{n,L}^{\text{SHO}}(p) = \frac{(-1)^n (-i)^L}{\beta^{3/2}} \sqrt{\frac{2n!}{\Gamma(n+L+\frac{3}{2})}} \left(\frac{p}{\beta} \right)^L e^{-p^2/2\beta^2} L_n^{L+\frac{1}{2}} \left(\frac{p^2}{\beta^2} \right),$$

where n and L are the radial and orbital angular momentum quantum numbers, respectively, and $L_n^{L+\frac{1}{2}}$ denotes an associated Laguerre polynomial.

The oscillator parameters for the charmed mesons and the hybrid are summarized in Table III. The values for β_ρ and β_λ are taken directly from the mass spectrum calculation, while the meson β parameters are determined by solving the Salpeter [32].

TABLE III. Oscillator parameters used in the decay width calculation.

Parameter	β_D	β_{D^*}	$\beta_{D(1P)}$	β_ρ	β_λ
Value (GeV)	0.574	0.496	0.385	0.432	0.625

With the wave functions fixed, the only remaining free parameter is the strong coupling constant g , related to the running coupling by $\alpha_S = g^2/(4\pi)$. Given that the constituent gluon mass is approximately 1 GeV, we adopt $\alpha_S = 0.5$ as a typical value of the running coupling at this energy scale.

We now examine the decay patterns for each member of the lowest hybrid multiplet, referring to the spectrum shown in Fig. 1.

- **0⁺ hybrid (4.189 GeV):** This state lies below all $S + P$ charmed meson thresholds. With no open decay channels satisfying the selection rules, its total width is expected to be very small. This makes the 0⁺ hybrid an excellent candidate for a narrow resonance.
- **1⁺ hybrid (4.231 GeV):** Despite lying above the $D\bar{D}_0^*(2300)$ threshold, this decay channel is forbidden by the exotic quantum numbers (1⁺ cannot couple to 0⁺ + 0⁻ in a relative S -wave). The $D\bar{D}^*$ channel is strongly suppressed by the spatial wave function overlap argument. Consequently, the 1⁺ charmonium hybrid is also predicted to be a narrow state, providing a clear experimental signature due to its exotic J^{PC} .
- **1⁻⁻ hybrid (4.276 GeV):** Decay to $D\bar{D}_0^*(2300)$ is forbidden by quantum numbers (1⁻⁻ cannot decay to 0⁺ + 0⁻ in a relative S -wave), and $D\bar{D}^*$ is suppressed. The predicted mass lies very close to the $D\bar{D}_1$ threshold, making the width extremely sensitive to the exact mass value. If $M_H > M_D + M_{D_1}$, the $D\bar{D}_1$ channel opens and becomes the dominant decay mode. Figure 2 shows the decay width as a function of mass, with the shaded band indicating ± 25 MeV theoretical uncertainty around our nominal value. The width varies from near zero below threshold to several tens of MeV above threshold.
- **2⁺ hybrid (4.316 GeV):** Decays to $D\bar{D}_0^*$ and $D\bar{D}_1$ proceed via D -waves, which strongly suppress these partial widths. The predicted mass is slightly below the $D\bar{D}_2^*$ threshold, so the mass dependence is again crucial. Figure 3 shows the decay width to $D\bar{D}_2^*$ as a function of mass. Once above threshold, this channel dominates, with contributions from $D\bar{D}_0^*$ and $D\bar{D}_1$ being negligible in comparison.

These distinctive decay patterns provide clear guidance for experimental searches. The 0⁺ and 1⁺ hybrids should appear as narrow resonances, with the 1⁺ being particularly distinctive due to its exotic quantum numbers. The 1⁻⁻ and 2⁺ states exhibit strong threshold effects, making them promising targets for scanning experiments at facilities such as BESIII, Belle II, and the Super Tau-Charm Facility. Precise measurement of their masses relative to the $D\bar{D}_1$ and $D\bar{D}_2^*$ thresholds would provide stringent tests of the hybrid interpretation.

IV. MORE SUGGESTION OF SEARCHING FOR THE DISCUSSED STATES

A. The 1⁻⁻ hybrid state

The 1⁻⁻ quantum numbers coincide with those of the photon, making e^+e^- annihilation an ideal production mechanism

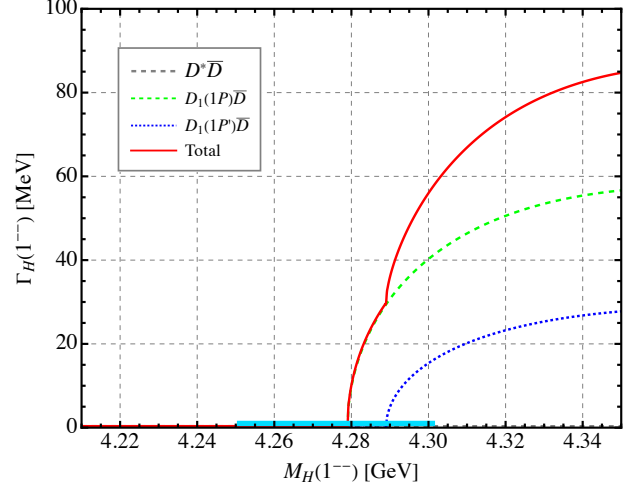


FIG. 2. Decay width of the 1⁻⁻ hybrid as a function of its mass. The shaded band on the mass axis indicates ± 25 MeV around our nominal value for the 1⁻⁻ hybrid mass. The vertical dashed line marks the $D\bar{D}_1$ threshold.

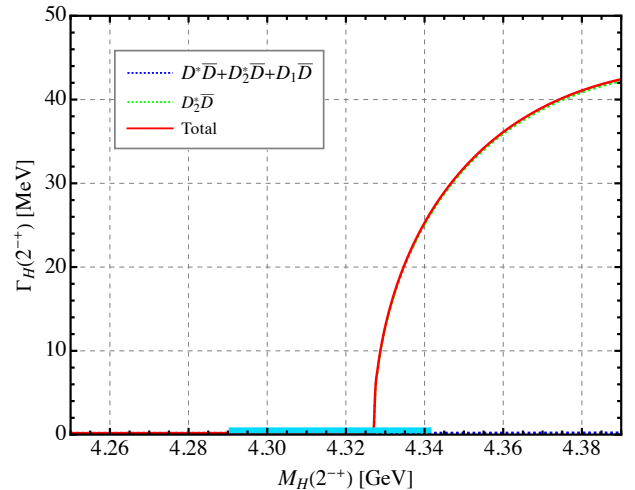


FIG. 3. Decay width of the 2⁺ hybrid as a function of its mass. The shaded band on the mass axis indicates ± 25 MeV around our nominal value for the 2⁺ hybrid mass. The vertical dashed line marks the $D\bar{D}_2^*$ threshold.

for this hybrid state. However, its coupling to the virtual photon is expected to be significantly smaller than that of conventional S -wave charmonium states because the hybrid's $c\bar{c}$ pair is in a spin-singlet configuration ($S_{c\bar{c}} = 0$), whereas the virtual photon couples preferentially to spin-triplet configurations. This coupling may nevertheless be larger than that of D -wave charmonium states. Given this suppressed direct production, distinguishing the hybrid from conventional charmonium relies critically on their distinct decay patterns.

Our calculation places the 1⁻⁻ hybrid mass at approximately 4.27 GeV, with a strong sensitivity of its decay width to the precise mass value. The state couples strongly to the $D\bar{D}_1$ channel, with a width reaching ~ 60 MeV near 4.3 GeV. If the mass lies below the $D\bar{D}_1$ threshold, two classes of de-

decay mechanisms remain available: (i) hidden-charm decays $H(1^{--}) \rightarrow (c\bar{c})(gg) \rightarrow c\bar{c} + \text{light hadrons}$, and (ii) annihilation decays $H(1^{--}) \rightarrow 3g \rightarrow \text{light hadrons}$ [37]. However, given the proximity of the predicted mass to the $D\bar{D}_1$ threshold and the strong coupling to this channel, the decay may proceed via an off-shell $D\bar{D}_1$ intermediate state:

$$H(1^{--}) \rightarrow D\bar{D}_1 \rightarrow D\bar{D}^*\pi,$$

which could become the dominant mode even when the $D\bar{D}_1$ threshold is not fully open. In this scenario, the state is expected to be relatively narrow.

The observed $Y(4230)$ resonance has long been considered a candidate for this 1^{--} hybrid state [38, 39], and its properties are broadly compatible with our predictions. Evidence supporting this interpretation includes: (i) its mass near 4.23 GeV is close to our calculated value, and (ii) its observed width of approximately 20 MeV and its detection in the $D\bar{D}^*\pi$ channel align with hybrid expectations.

However, recent precise experimental data present challenges to the pure hybrid assignment for $Y(4230)$. First, the 1^{--} hybrid has $S_{c\bar{c}} = 0$, so heavy quark spin symmetry suppresses hidden-charm decays into final states involving charmonia with $S_{c\bar{c}} = 1$. Yet experimental measurements yield [40]

$$\mathcal{R} = \frac{\text{BR}(Y(4230) \rightarrow J/\psi\pi\pi)}{\text{BR}(Y(4230) \rightarrow h_c\pi\pi)} \approx 2, \quad (28)$$

which clearly contradicts this symmetry expectation. Second, BESIII has recently observed $Y(4230)$ in the $e^+e^- \rightarrow D\bar{D}$ channel [41], contradicting the predicted vanishing width for a TE hybrid decaying into $D\bar{D}$. These tensions suggest that interpreting $Y(4230)$ as a pure hybrid state remains problematic. The discrepancies might be resolved by including additional mechanisms, such as mixing between the hybrid and conventional charmonium states with nearby masses.

B. The $(0, 1, 2)^{++}$ hybrid states

In the light-flavor sector, several candidates for hybrid mesons with exotic quantum numbers $J^{PC} = 1^{++}$ have been proposed, including $\pi_1(1400)$, $\pi_1(1600)$, $\pi_1(2015)$, and the more recent $\eta_1(1855)$. The π_1 states have been observed in diffractive πN scattering processes [1–10, 13, 14] and in $N\bar{N}$ annihilation [4, 12, 42]. Such production mechanisms are not directly applicable to charmonium hybrids. Notably, the $\eta_1(1855)$ was discovered in the radiative annihilation process $J/\psi \rightarrow \gamma\eta_1(1855)$ [15, 16]. This is significant because quarkonium annihilation provides a gluon-rich environment, making it an ideal laboratory for producing hybrid states.

For a 1^{--} bottomonium state such as $\Upsilon(nS)$, one of the dominant annihilation processes proceeds via γgg intermediate states (see Fig. 4). The subsequent hadronization of this gluonic system can produce charmonium hybrids. Crucially, the production of conventional charmonium in such processes requires the simultaneous creation of two $c\bar{c}$ pairs, since the $c\bar{c}$

pair produced directly from gluons is in a color-octet configuration and must neutralize its color. This additional suppression makes hybrid production comparatively more favorable in quarkonium annihilation. Annihilation decays of $\Upsilon(nS)$ states,

$$\Upsilon(nS) \rightarrow \gamma H_{c\bar{c}} \quad \text{and} \quad \Upsilon(nS) \rightarrow X H_{c\bar{c}},$$

where X denotes one or more light hadrons, therefore offer a promising pathway to produce hybrid states with quantum numbers $J^{PC} = (0, 1, 2)^{++}$. The presence of a photon in the final state selects $C = +1$ hybrids, precisely the $(0, 1, 2)^{++}$ multiplet.

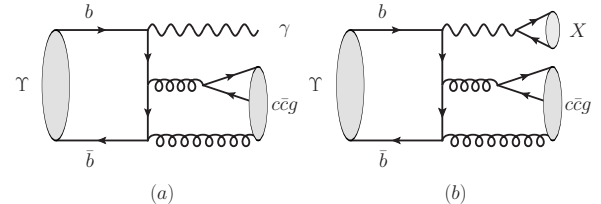


FIG. 4. Production of a charmonium hybrid through annihilation decay of Υ states: (a) $\gamma H_{c\bar{c}}$ and (b) $X H_{c\bar{c}}$, where X denotes possible single or multiple hadrons.

The decays of $(0, 1, 2)^{++}$ charmonium hybrids may proceed via two mechanisms: hidden-charm decays $H(J^{++}) \rightarrow (c\bar{c})(gg) \rightarrow c\bar{c} + \text{light hadrons}$, and annihilation decays $H(J^{++}) \rightarrow 2g \rightarrow \text{light hadrons}$. These modes may have sizable branching fractions, particularly for the 0^{++} and 1^{++} states whose decays to $S + P$ charmed meson pairs are forbidden either by quantum numbers or by phase space.

For hidden-charm decays, the final-state charmonium must have the same C -parity as the hybrid because the gg system has even C -parity. Heavy-quark spin symmetry further favors $S_{c\bar{c}} = 1$ in the transition. These constraints select hidden-charm decays involving χ_{cJ} states:

$$H(J^{++}) \rightarrow \chi_{cJ}\pi\pi, \chi_{cJ}K\bar{K}, \dots$$

For annihilation decays into light hadrons, many final states are possible, and the decay pattern may resemble that of the η_c , as both proceed via gg annihilation.

The 2^{++} charmonium hybrid is particularly interesting. Our calculated mass lies very close to the $D\bar{D}_2^*(2460)$ threshold. Consequently, the $D\bar{D}_2^*(2460)$ and its subsequent decay $D\bar{D}^{(*)}\pi$ channels are a promising discovery mode if the mass lies above the corresponding thresholds. Moreover, the proximity to this threshold implies that rescattering effects into hidden-charm final states could be significant. Heavy-quark spin symmetry restricts the $c\bar{c}$ pair to $S_{c\bar{c}} = 1$, making processes such as

$$H(2^{++}) \rightarrow D\bar{D}_2^*(2460) \rightarrow J/\psi\omega, J/\psi\phi$$

promising channels for experimental searches. Therefore, $\Upsilon \rightarrow \gamma J/\psi\omega(\phi)$ and $\Upsilon \rightarrow X J/\psi\omega(\phi)$ decays provide particularly clean signatures. Future high-luminosity B -factories, such as Belle II, are well positioned to explore these decay channels and potentially discover the 2^{++} charmonium hybrid.

V. SUMMARY

Charmonium hybrids offer a unique window into the gluonic degrees of freedom in QCD. In this work, we have systematically investigated the spectrum and decay properties of charmonium hybrid mesons within a constituent gluon model, treating the hybrid as a $c\bar{c}g$ three-body system with a TE mode gluon. Our calculations yield masses for the lowest hybrid multiplet: 4.189 GeV (0^+), 4.231 GeV (1^+), 4.276 GeV (1^{--}), and 4.316 GeV (2^+). These states lie in the 4.2–4.3 GeV region, in close proximity to several important charmed meson pair thresholds.

The two-body open-charm decays of these hybrids were calculated using the QCD quark-gluon coupling mechanism. The dominant decay modes are to S -wave plus P -wave charmed meson pairs, a consequence of the selection rule that forbids decays into two mesons with identical spatial wave functions. The 1^{--} hybrid decays predominantly to $D\bar{D}_1$ when kinematically allowed, with a width that exhibits strong mass dependence near threshold. The 2^+ hybrid favors $D\bar{D}_2^*$ decay when phase space permits. The 0^+ and 1^+ hybrids are expected to be narrow states due to phase space limitations and quantum number constraints.

The mass and decay properties of the $Y(4230)$ resonance show reasonable agreement with our predicted 1^{--} hybrid. However, recent experimental data on its hidden-charm decays and $D\bar{D}$ production challenge a pure hybrid interpretation. This tension suggests that more complex scenarios, such as mixing between hybrid and conventional charmonium states, may be necessary to fully reconcile theory with observation.

The $(0, 1, 2)^+$ hybrids present promising discovery opportunities in Υ annihilation decays, specifically through $\Upsilon \rightarrow \gamma H_{c\bar{c}}$ and $\Upsilon \rightarrow X H_{c\bar{c}}$ channels. Their distinctive decay patterns, combined with heavy-quark spin symmetry constraints, provide powerful tools for distinguishing hybrids from conventional charmonium states. The 0^+ and 1^+ hybrids may be observable as narrow resonances in hidden-charm channels such as $\chi_{cJ}\pi\pi$ and $\chi_{cJ}K\bar{K}$. The 2^+ hybrid may be accessible through its direct decay to $D\bar{D}_2^*$ and $D\bar{D}^{(*)}\pi$, or via rescattering of the $D\bar{D}_2^*$ channel into hidden-charm final states like $J/\psi\omega$ and $J/\psi\phi$.

In conclusion, charmonium hybrids constitute a unique laboratory for exploring gluonic excitations in QCD. The theoretical predictions presented here, combined with ongoing and future experimental efforts at BESIII, Belle II, and next-generation facilities, offer promising prospects for the discovery and characterization of these exotic hadrons. A combined analysis of multiple decay channels and production mechanisms will be essential to establish the hybrid nature of any observed candidate.

ACKNOWLEDGMENTS

This work is also supported by the Nation Natural Science Foundation of China under Grants No. 12335001 and No. 12247101, the 111 Center under Grant No. B20063,

the Natural Science Foundation of Gansu Province (No. 22JR5RA389, No. 25JRRA799), the Talent Scientific Fund of Lanzhou University, the fundamental Research Funds for the Central Universities (No. lzujbky-2023-stlt01), the project for top-notch innovative talents of Gansu province and Lanzhou City High-Level Talent Funding.

Appendix A: The TE and TM gluons

The gluon spin couples to its orbital angular momentum l_g to yield the total gluon angular momentum j_g . The gluon wave function is an eigenstate of \hat{J}_g^2 , \hat{J}_{gz} , \hat{L}_g^2 and \hat{S}_g^2 , and can be expressed in terms of the vector spherical harmonics

$$Y_{j_g, m_g}^{l_g}(\theta, \phi) \equiv \sum_{m_{l_g}, \sigma} \langle lm_l; 1\sigma | j_g m_g \rangle Y_{j_g, m_{l_g}}(\theta, \phi) \epsilon(\sigma), \quad (A1)$$

where $\epsilon(\sigma)$ is the gluon polarization function. The transverse and longitudinal components can be separated as follows [43]:

$$\begin{aligned} Y_{j_g, m_g}^{(\text{TE})} &= Y_{j_g, m_g}^{j_g}, \\ Y_{j_g, m_g}^{(\text{TM})} &= \sqrt{\frac{j_g + 1}{2j_g + 1}} Y_{j_g, m_g}^{j_g-1} + \sqrt{\frac{j_g}{2j_g + 1}} Y_{j_g, m_g}^{j_g+1}, \\ Y_{j_g, m_g}^{(\text{long})} &= \sqrt{\frac{j_g}{2j_g + 1}} Y_{j_g, m_g}^{j_g-1} - \sqrt{\frac{j_g + 1}{2j_g + 1}} Y_{j_g, m_g}^{j_g+1}, \end{aligned}$$

where the TE and TM spherical harmonics satisfy $\hat{n} \cdot Y_{j_g, m_g}^{(\text{TE/TM})} = 0$ and the longitudinal spherical harmonics satisfy $\hat{n} \times Y_{j_g, m_g}^{(\text{long})} = 0$, with \hat{n} the unit vector in the (θ, ϕ) direction. These spherical harmonics are mutually orthogonal. Expressing the gluon polarization in the helicity basis via $\epsilon(\sigma) = D_{\sigma, \lambda}^{1*}(\phi, \theta, 0) \epsilon(\lambda, \hat{n})$ and reducing two Wigner- D matrices to one gives

$$\begin{aligned} Y_{j_g, m_g}^{(\text{TE})}(\theta, \phi) &= \sqrt{\frac{2j_g + 1}{8\pi}} (D_{m_g, -1}^{j_g*}(\phi, \theta, 0) \epsilon(-1, \hat{n}) \\ &\quad - D_{m_g, 1}^{j_g*}(\phi, \theta, 0) \epsilon(1, \hat{n})), \end{aligned} \quad (A2)$$

$$\begin{aligned} Y_{j_g, m_g}^{(\text{TM})}(\theta, \phi) &= \sqrt{\frac{2j_g + 1}{8\pi}} (D_{m_g, 1}^{j_g*}(\phi, \theta, 0) \epsilon(-1, \hat{n}) \\ &\quad + D_{m_g, -1}^{j_g*}(\phi, \theta, 0) \epsilon(-1, \hat{n})). \end{aligned} \quad (A3)$$

The above expression can be rewritten as:

$$Y_{j_g, m_g}^{(\xi)}(\theta, \phi) = \sqrt{\frac{2j_g + 1}{4\pi}} D_{m_g, \mu}^{j_g*}(\phi, \theta, 0) \chi_{\mu, \lambda}^{(\xi)} \epsilon(\lambda, \hat{n}), \quad (A4)$$

where $\xi = -1$ corresponds to a TE gluon and $\xi = 1$ corresponds to a TM gluon. The explicit form of $\chi_{\lambda, \mu}^{(\xi)}$ is

$$\chi_{\lambda, \mu}^{(-)} = -\frac{\lambda}{\sqrt{2}} \delta_{\lambda, \mu}, \quad \chi_{\lambda, \mu}^{(+)} = \frac{1}{\sqrt{2}} \delta_{\lambda, \mu}. \quad (A5)$$

Appendix B: The field theory convention and decay amplitude

In deriving the decay amplitude, we have adopted the following field theory convention. The spinor field have the form

$$\begin{aligned}\psi(x) &= \sum_{s=1}^2 \int \frac{d^3 p}{(2\pi)^{3/2}} \frac{1}{\sqrt{2E_p}} (b_{\mathbf{p},s} u_{\mathbf{p}}^s e^{-ipx} + d_{\mathbf{p},s}^\dagger v_{\mathbf{p}}^s e^{ipx}), \\ \bar{\psi}(x) &= \sum_{s=1}^2 \int \frac{d^3 p}{(2\pi)^{3/2}} \frac{1}{\sqrt{2E_p}} (d_{\mathbf{p},s} \bar{v}_{\mathbf{p}}^s e^{-ipx} + b_{\mathbf{p},s}^\dagger \bar{u}_{\mathbf{p}}^s e^{ipx})\end{aligned}\quad (\text{B1})$$

where the spinors are given in the Dirac representation by

$$u(p, s) = \sqrt{E + m} \begin{pmatrix} \chi_s \\ \sigma_{\mathbf{p}} \chi_s \end{pmatrix}, v(p, s) = \sqrt{E + m} \begin{pmatrix} \sigma_{\mathbf{p}} \tilde{\chi}_s \\ \tilde{\chi}_s \end{pmatrix} \quad (\text{B2})$$

where the χ_s is the quark spinor and $\tilde{\chi}_{s'} = -i\sigma_2 \chi_{s'}^*$ is the antiquark spinor. The creation and annihilation operators obey the anticommutation rules

$$\{b_{\mathbf{p},s}, b_{\mathbf{q},s'}^\dagger\} = \{d_{\mathbf{p},s}, d_{\mathbf{q},s'}^\dagger\} = \delta^{(3)}(\mathbf{p} - \mathbf{q}) \delta_{s,s'}, \quad (\text{B3})$$

with all other anticommutators equal to zero. Then the equal time anticommutation relation for the ψ and ψ^\dagger are

$$\begin{aligned}\{\psi_a(\mathbf{x}), \psi_b^\dagger(\mathbf{y})\} &= \delta^{(3)}(\mathbf{x} - \mathbf{y}) \delta_{a,b}, \\ \{\psi_a(\mathbf{x}), \psi_b(\mathbf{y})\} &= \{\psi_a^\dagger(\mathbf{x}), \psi_b^\dagger(\mathbf{y})\} = 0.\end{aligned}\quad (\text{B4})$$

The normalization condition for the single particle state created by the creation oprators is then

$$\langle \mathbf{p}, s | \mathbf{q}, s' \rangle = \langle 0 | \{b_{\mathbf{p},s}, b_{\mathbf{q},s'}^\dagger\} | 0 \rangle = \delta^{(3)}(\mathbf{p} - \mathbf{q}) \delta_{s,s'} \quad (\text{B5})$$

Similarly, the gluon field have the form

$$\begin{aligned}A_a^\mu(x) &= \sum_{\lambda=1}^2 \int \frac{d^3 k}{(2\pi)^{3/2}} \frac{1}{\sqrt{2\omega_k}} (a_{\mathbf{k},\lambda,a} \epsilon^\mu(\mathbf{k}, \lambda) e^{-ikx} \\ &\quad + a_{\mathbf{k},\lambda,a}^\dagger \epsilon^{\mu*}(\mathbf{k}, \lambda) e^{ikx}).\end{aligned}\quad (\text{B6})$$

The gluon state created by the creation operator is normalized in the same way as the quark state.

In these conventions, the decay amplitude is related to the matrix element of the interaction Hamiltonian H_I as

$$\langle BC | H_I | H \rangle = (2\pi) \delta^{(4)}(P_B + P_C - P_H) \mathcal{M}(\mathbf{P}). \quad (\text{B7})$$

Using the interaction Hamiltonian in Eq. (16), the hybrid and

meson states, the decay amplitude can be derived as follows:

$$\begin{aligned}&(2\pi) \delta^{(4)}(P_B + P_C - P_H) \mathcal{M}(\mathbf{P}) \\ &= \left[\int d^3 p_{B_1} d^3 p_{B_2} d^3 p_{C_1} d^3 p_{C_2} \delta^{(3)}(\mathbf{p}_{B_1} + \mathbf{p}_{B_2} - \mathbf{P}) \right. \\ &\quad \times \delta^{(3)}(\mathbf{p}_{C_1} + \mathbf{p}_{C_2} - \mathbf{P}_C) \dots \left. \right] \\ &\quad \times \left[g \int \frac{d^3 p d^3 p' d^3 k'}{(2\pi)^{9/2}} (2\pi)^4 \delta^{(4)}(p + p' - k') \dots \right] \\ &\quad \times \left[\int d^3 p_1 d^3 p_2 d^3 k \delta^{(3)}(\mathbf{p}_1 + \mathbf{p}_2 + \mathbf{k}) \dots \right] \\ &\quad \times \langle \mathbf{p}_{B_1} \mathbf{p}_{B_2}; \mathbf{p}_{C_1} \mathbf{p}_{C_2} | b_{\mathbf{p}}^\dagger d_{\mathbf{p}'}^\dagger a_{\mathbf{k}'} | \mathbf{p}_1 \mathbf{p}_2 \mathbf{k} \rangle \\ &= g \int d^3 p_1 d^3 p_2 d^3 k \frac{(2\pi)^4}{(2\pi)^{9/2}} \delta^{(4)}(P_B - p_1 + P_C - p_2 - k) \\ &\quad \times \delta^{(4)}(\mathbf{p}_1 + \mathbf{p}_2 + \mathbf{k}) \dots \\ &= (2\pi) \delta^{(4)}(P_B + P_C - P_H) \frac{g}{(2\pi)^{3/2}} \int d^3 q d^3 k \dots\end{aligned}$$

where the ellipses represent the wave functions and spinor structures in the integrand. The final expression of the decay amplitude is given in Eq. (23).

Appendix C: The derivation of $\chi_s^\dagger \sigma \tilde{\chi}_{s'} \cdot \epsilon(\lambda, \mathbf{k})$

Here, the detailed derivation of Eq. (24) is given. First, we note that

$$\begin{aligned}\chi_\sigma^\dagger S \chi_{\sigma'} \cdot \epsilon(\lambda, \mathbf{k}) &= \sum_\mu \chi_\sigma^\dagger S_{\mu\sigma'} \chi_{\sigma'} D_{\mu,\lambda}^1(\hat{\mathbf{k}}) \\ &= \sum_\mu \frac{\sqrt{3}}{2} \langle \frac{1}{2}\sigma'; 1\mu | \frac{1}{2}\sigma \rangle D_{\mu,\lambda}^1(\hat{\mathbf{k}}) \\ &= -\text{sign}(-\sigma') \frac{1}{2} \sqrt{2}^{|s-\sigma'|} D_{\sigma-\sigma',\lambda}^1(\hat{\mathbf{k}})\end{aligned}\quad (\text{C1})$$

In the meanwhile, we have

$$\tilde{\chi}_{s'} = -i\sigma_2 \chi_{s'}^* = \text{sign}(s') \chi_{-s'} \quad (\text{C2})$$

Combining the above two equation, we get

$$\chi_s^\dagger \sigma \tilde{\chi}_{s'} \cdot \epsilon(\lambda, \mathbf{k}) = -\sqrt{2}^{|s+s'|} D_{s+s',\lambda}^1(\hat{\mathbf{k}}) \quad (\text{C3})$$

Appendix D: The convention of S -matrix and decay width

The explicit formula of decay width depends on the convention of S -matrix and normalization of states. Here we summarize the nonrelativistic convention used in this work. The S -matrix is defined as

$$\langle \mathbf{p}_B \mathbf{p}_C | S^{NR} | \mathbf{p}_A \rangle = \langle \mathbf{p}_B \mathbf{p}_C | \mathbf{p}_A \rangle - 2\pi i \delta^{(4)}(p_A - p_B - p_C) \mathcal{M}_{A \rightarrow BC}, \quad (\text{D1})$$

where the normalization of the single particle state is

$$\langle \mathbf{p} | \mathbf{p}' \rangle = \delta^{(3)}(\mathbf{p} - \mathbf{p}') \quad (\text{D2})$$

Note that in the standard relativistic convention [44], the normalization of single particle state and S -matrix are

$$\begin{aligned} {}_R\langle \mathbf{p}|\mathbf{p}'\rangle_R &= (2\pi)^3(2E_p)\delta^{(3)}(\mathbf{p}-\mathbf{p}'), \\ {}_R\langle \mathbf{p}_B\mathbf{p}_C|S^R|\mathbf{p}_A\rangle_R &= {}_R\langle \mathbf{p}_B\mathbf{p}_C|\mathbf{p}_A\rangle_R \\ &\quad +i(2\pi)^4\delta^{(4)}(p_A-p_B-p_C)T_{A\rightarrow BC} \end{aligned} \quad (D3)$$

The two-body decay width is given by

$$\Gamma_{A\rightarrow BC} = \frac{P}{8\pi m_A^2} \frac{1}{2J_A+1} \sum_{\text{spin}} |T_{A\rightarrow BC}|^2, \quad (D4)$$

where P is the momentum of the final state particles in the rest frame of particle A . The S -matrix in the two conventions differ by a factor that can be determined by their different normalization condition of particle states. The relation between the nonrelativistic amplitude $\mathcal{M}_{A\rightarrow BC}$ and the relativistic amplitude $T_{A\rightarrow BC}$ is

$$(2\pi)^4 T_{A\rightarrow BC} = -(2\pi) \prod_{i=A,B,C} \left[(2\pi)^{3/2} \sqrt{2E_i} \right] \mathcal{M}_{A\rightarrow BC} \quad (D5)$$

- [1] H. Aoyagi *et al.*, Study of the $\eta\pi^-$ system in the π^-p reaction at 6.3 GeV/c, *Phys. Lett. B* **314**, 246 (1993).
- [2] D. R. Thompson *et al.* (E852), Evidence for exotic meson production in the reaction $\pi^-p \rightarrow \eta\pi^-p$ at 18 GeV/c, *Phys. Rev. Lett.* **79**, 1630 (1997), arXiv:hep-ex/9705011.
- [3] G. S. Adams *et al.* (E852), Observation of a new $J^{PC} = 1^{++}$ exotic state in the reaction $\pi^-p \rightarrow \pi^+\pi^-\pi^-p$ at 18 GeV/c, *Phys. Rev. Lett.* **81**, 5760 (1998).
- [4] A. Abele *et al.* (Crystal Barrel), Exotic $\eta\pi$ state in $\bar{p}d$ annihilation at rest into $\pi^-\pi^0\eta p$ (spectator), *Phys. Lett. B* **423**, 175 (1998).
- [5] D. Alde *et al.* (IHEP-IISN-LANL-LAPP), Evidence for a 1^{++} Exotic Meson, *Phys. Lett. B* **205**, 397 (1988).
- [6] Y. A. Khokhlov (VES), Study of $X(1600)$ 1^{++} hybrid, *Nucl. Phys. A* **663**, 596 (2000).
- [7] V. Dorofeev *et al.* (VES), The $J^{PC} = 1^{++}$ hunting season at VES, *AIP Conf. Proc.* **619**, 143 (2002), arXiv:hep-ex/0110075.
- [8] C. A. Baker *et al.*, Confirmation of $a_0(1450)$ and $\pi_1(1600)$ in $\bar{p}p \rightarrow \omega\pi^+\pi^-\pi^0$ at rest, *Phys. Lett. B* **563**, 140 (2003).
- [9] M. Alekseev *et al.* (COMPASS), Observation of a $J^{PC} = 1^{++}$ exotic resonance in diffractive dissociation of 190 GeV/c π^- into $\pi^-\pi^+\pi^+$, *Phys. Rev. Lett.* **104**, 241803 (2010), arXiv:0910.5842 [hep-ex].
- [10] G. S. Adams *et al.* (CLEO), Amplitude analyses of the decays $\chi_{c1} \rightarrow \eta\pi^+\pi^-$ and $\chi_{c1} \rightarrow \eta'\pi^+\pi^-$, *Phys. Rev. D* **84**, 112009 (2011), arXiv:1109.5843 [hep-ex].
- [11] A. Rodas *et al.* (JPAC), Determination of the pole position of the lightest hybrid meson candidate, *Phys. Rev. Lett.* **122**, 042002 (2019), arXiv:1810.04171 [hep-ph].
- [12] M. Albrecht *et al.* (Crystal Barrel), Coupled channel analysis of $\bar{p}p \rightarrow \pi^0\eta$, $\pi^0\eta\eta$ and $K^+K^-\pi^0$ at 900 MeV/c and of $\pi\pi$ -scattering data, *Eur. Phys. J. C* **80**, 453 (2020), arXiv:1909.07091 [hep-ex].
- [13] J. Kuhn *et al.* (E852), Exotic meson production in the $f_1(1285)\pi^-$ system observed in the reaction $\pi^-p \rightarrow \eta\pi^+\pi^-\pi^-p$ at 18 GeV/c, *Phys. Lett. B* **595**, 109 (2004), arXiv:hep-ex/0401004.
- [14] M. Lu *et al.* (E852), Exotic meson decay to $\omega\pi^0\pi^-$, *Phys. Rev. Lett.* **94**, 032002 (2005), arXiv:hep-ex/0405044.
- [15] M. Ablikim *et al.* (BESIII), Partial wave analysis of $J/\psi \rightarrow \gamma\eta\eta'$, *Phys. Rev. D* **106**, 072012 (2022), [Erratum: Phys. Rev. D 107, 079901 (2023)], arXiv:2202.00623 [hep-ex].
- [16] M. Ablikim *et al.* (BESIII), Observation of an Isoscalar Resonance with Exotic $J^{PC} = 1^{++}$ Quantum Numbers in $J/\psi \rightarrow \gamma\eta\eta'$, *Phys. Rev. Lett.* **129**, 192002 (2022), [Erratum: Phys. Rev. Lett. 130, 159901 (2023)], arXiv:2202.00621 [hep-ex].
- [17] F.-Y. Zhang, Q. Huang, and L.-M. Wang, Spectral analysis and decay mechanisms of 1^{++} hybrid states in light meson sector, *Phys. Rev. D* **113**, 014002 (2026), arXiv:2503.01443 [hep-ph].
- [18] Z.-X. Ma, Q. Huang, R. Chen, L.-M. Wang, Y. Tan, X.-H. Hu, J. He, and H.-X. Huang, Proper constituent gluon mass as the final piece to construct hybrid mesons, *Phys. Rev. D* **112**, L111503 (2025), arXiv:2504.05818 [hep-ph].
- [19] T. Barnes, F. E. Close, and E. S. Swanson, Hybrid and conventional mesons in the flux tube model: Numerical studies and their phenomenological implications, *Phys. Rev. D* **52**, 5242 (1995), arXiv:hep-ph/9501405.
- [20] S.-L. Zhu, Masses and decay widths of heavy hybrid mesons, *Phys. Rev. D* **60**, 014008 (1999), arXiv:hep-ph/9812405.

Then we obtain the decay width in terms of the nonrelativistic amplitude:

$$\Gamma_{A\rightarrow BC} = \frac{8\pi^2}{m_A} E_B E_C \frac{P}{2J_A+1} \sum_{\text{spin}} |\mathcal{M}_{A\rightarrow BC}|^2. \quad (D6)$$

The above amplitude can be expressed in terms of the partial wave amplitude as

$$\begin{aligned} &\mathcal{M}^{M_A, M_B, M_C}(\mathbf{P}) \\ &= \sum_{\substack{L, S \\ M_S, M_L}} \langle LM_L S M_S | J_A M_A \rangle \langle J_B M_B J_C M_C | S M_S \rangle \\ &\quad \times Y_{LM_L}(\hat{\mathbf{P}}) \mathcal{M}^{LS}(P). \end{aligned} \quad (D7)$$

From the above relation, we can get

$$\sum_{M_{J_A}, M_{J_B}, M_{J_C}} |\mathcal{M}^{M_{J_A}, M_{J_B}, M_{J_C}}(\mathbf{P})|^2 = \sum_{L, S} \frac{2J_A+1}{4\pi} |\mathcal{M}^{LS}(P)|^2,$$

so the decay width in terms of the partial wave amplitude is

$$\Gamma_{A\rightarrow BC} = 2\pi \frac{E_B E_C}{m_A} P \sum_{L, S} |\mathcal{M}^{LS}(P)|^2. \quad (D8)$$

This is the formula used in the main text.

- [21] Y. S. Kalashnikova and A. V. Nefediev, Spectra and decays of hybrid charmonia, *Phys. Rev. D* **77**, 054025 (2008), arXiv:0801.2036 [hep-ph].
- [22] W. Chen, R. T. Kleiv, T. G. Steele, B. Bulthuis, D. Harnett, J. Ho, T. Richards, and S.-L. Zhu, Mass Spectrum of Heavy Quarkonium Hybrids, *JHEP* **09**, 019, arXiv:1304.4522 [hep-ph].
- [23] Y. S. Kalashnikova and A. V. Nefediev, QCD string in excited heavy-light mesons and heavy-quark hybrids, *Phys. Rev. D* **94**, 114007 (2016), arXiv:1611.10066 [hep-ph].
- [24] R. Oncala and J. Soto, Heavy Quarkonium Hybrids: Spectrum, Decay and Mixing, *Phys. Rev. D* **96**, 014004 (2017), arXiv:1702.03900 [hep-ph].
- [25] C. Farina, H. Garcia Tecocoatzi, A. Giachino, E. Santopinto, and E. S. Swanson, Heavy hybrid decays in a constituent gluon model, *Phys. Rev. D* **102**, 014023 (2020), arXiv:2005.10850 [hep-ph].
- [26] P. R. Page, Why hybrid meson coupling to two S -wave mesons is suppressed, *Phys. Lett. B* **402**, 183 (1997), arXiv:hep-ph/9611375.
- [27] N. Isgur and J. E. Paton, A Flux Tube Model for Hadrons in QCD, *Phys. Rev. D* **31**, 2910 (1985).
- [28] F. E. Close and P. R. Page, The Production and decay of hybrid mesons by flux tube breaking, *Nucl. Phys. B* **443**, 233 (1995), arXiv:hep-ph/9411301.
- [29] Y. S. Kalashnikova and D. S. Kuzmenko, Hybrid adiabatic potentials in the QCD string model, *Phys. Atom. Nucl.* **66**, 955 (2003), arXiv:hep-ph/0203128.
- [30] D. Horn and J. Mandula, A Model of Mesons with Constituent Gluons, *Phys. Rev. D* **17**, 898 (1978).
- [31] E. S. Swanson and A. P. Szczepaniak, Heavy hybrids with constituent gluons, *Phys. Rev. D* **59**, 014035 (1999), arXiv:hep-ph/9804219.
- [32] B. Chen and X. Liu, Investigating hybrid mesons with 0^{+-} and 2^{+-} exotic quantum numbers, *Eur. Phys. J. C* **85**, 788 (2025), arXiv:2503.06116 [hep-ph].
- [33] T. Barnes, F. E. Close, and F. de Viron, Q \bar{Q} G Hermaphrodite Mesons in the MIT Bag Model, *Nucl. Phys. B* **224**, 241 (1983).
- [34] L. Liu, G. Moir, M. Peardon, S. M. Ryan, C. E. Thomas, P. Vilaseca, J. J. Dudek, R. G. Edwards, B. Joo, and D. G. Richards (Hadron Spectrum), Excited and exotic charmonium spectroscopy from lattice QCD, *JHEP* **07**, 126, arXiv:1204.5425 [hep-ph].
- [35] G. K. C. Cheung, C. O'Hara, G. Moir, M. Peardon, S. M. Ryan, C. E. Thomas, and D. Tims (Hadron Spectrum), Excited and exotic charmonium, D_s , and D meson spectra for two light quark masses from lattice QCD, *JHEP* **12**, 089, arXiv:1610.01073 [hep-lat].
- [36] K. J. Juge, J. Kuti, and C. Morningstar, Fine structure of the QCD string spectrum, *Phys. Rev. Lett.* **90**, 161601 (2003), arXiv:hep-lat/0207004.
- [37] F. E. Close and S. Godfrey, Charmonium hybrid production in exclusive B meson decays, *Phys. Lett. B* **574**, 210 (2003), arXiv:hep-ph/0305285.
- [38] S.-L. Zhu, The Possible interpretations of $Y(4260)$, *Phys. Lett. B* **625**, 212 (2005), arXiv:hep-ph/0507025.
- [39] F. E. Close and P. R. Page, Gluonic charmonium resonances at BaBar and BELLE?, *Phys. Lett. B* **628**, 215 (2005), arXiv:hep-ph/0507199.
- [40] S. Navas *et al.* (Particle Data Group), Review of particle physics, *Phys. Rev. D* **110**, 030001 (2024).
- [41] M. Ablikim *et al.* (BESIII), Precise Measurement of Born Cross Sections for $e^+e^- \rightarrow D\bar{D}$ at $\sqrt{s} = 3.80 - 4.95$ GeV, *Phys. Rev. Lett.* **133**, 081901 (2024), arXiv:2402.03829 [hep-ex].
- [42] A. Abele *et al.* (Crystal Barrel), Evidence for a $\pi\eta$ P wave in $\bar{p}p$ annihilations at rest into $\pi^0\pi^0\eta$, *Phys. Lett. B* **446**, 349 (1999).
- [43] D. A. Varshalovich, A. N. Moskalev, and V. K. Khersonskii, *Quantum Theory of Angular Momentum* (WORLD SCIENTIFIC, 1988) <https://www.worldscientific.com/doi/pdf/10.1142/0270>.
- [44] M. E. Peskin and D. V. Schroeder, *An Introduction to quantum field theory* (Addison-Wesley, Reading, USA, 1995).